Refractive Index Estimation of Naturally Occurring Surfaces Using Photometric Stereo

Gule Saman and Edwin R. Hancock*

Department of Computer Science, University of York, YO10 5GH, UK

Abstract. This paper describes a novel approach to the computation of refractive index from polarisation information. Specifically, we use the refractive index measurements to gauge the quality of fruits and vegetables. We commence by using the method of moments to estimate the components of the polarisation image computed from intensity images acquired by employing multiple polariser angles. The method uses photometric stereo to estimate surface normals and then uses the estimates of surface normal, zenith angle and polarisation measurements to estimate the refractive index. The method is applied to surface inspection problems. Experiments on fruits and vegetables at different stages of decay illustrate the utility of the method in assessing surface quality.

Keywords: Refractive index estimation, Photometric stereo, Polarisation Information, Fresnel Theory.

1 Introduction

The physics of light has been widely exploited for surface inspection problems. Although the majority of methods make use of images in the visble, infra-red or ultraviolet ranges, there is a wealth of additional information that can be exploited including the pattern of light scattering, multispectral signatures and polarisation. In fact, the optical properties of surfaces prove to be particularly useful for assessing the quality of changes in naturally occurring surfaces. Here the scattering properties of visible light have been explioted for acquiring morphological information about the tissues. The two factors that effect the scattering of light from biological surfaces are, tissue morphology and biochemistry. Morphology affects the distribution of the scattered light, while the refractive index is determined by the biochemical composition of the tissue [1]. The refractive index is the ratio of the speed of light in vacuum to that in the material, and it hence determines the light transmission properties of a material. To understand the detailed propagation in biological tissue consisting of cells, the Mie theory has been used for approximating the scattering of light assuming that the cells are unifomrly sized homogeneous spheres [2]. A more complex approach is provied by the finite-difference time-domain (FDTD) model where Maxwell's equations are used for modelling the scattering of light from biological cells [3].

Refractive index therefore plays an important role in characterising the properties of biological tissue. One way of measuring refractive index is to turn to the Fresnel

* Edwin Hancock is supported by the EU FET project SIMBAD and by a Royal Society Wolfson Research Merit Award.

G. Maino and G.L. Foresti (Eds.): ICIAP 2011, Part I, LNCS 6978, pp. 267–275, 2011.

theorty and to use polarisation measurements. Polarisation information has been used for developing algorithms for a diverse set of problems in computer vision ranging from surface inspection to surface reconstruction. The Fresnel theory is used to determine the parallel and perpendicular components of the electric field for incident light in order to, model the transmission and reflection of these components [4]. The Fresnel theory of light has been used by Wolff [5] for developing a polarisation based method for identifying metal surfaces and dielectrics. It can be applied at a smooth boundary between two media as a quantitative measure of reflection and refraction of incident light [4,6]. Generally speaking, modeling dielectrics is straightforward as compared to modeling metals, since in the latter case the incident electromagnetic field induces surface currents for which the Fresnel theory alone is insufficient. When dealing with dielectrics, it is convenient to distinguish between the specular and diffuse polarisation. In specular polarisation, polarised incident light is reflected from the reflecting surface where the orientation of the surface determines the plane of polarisation. In diffuse polarisation, unpolarised incident light is subjected to subsurface scattering before being re-emitted hence spontaneously acquiring polarisation[5].

A polaroid filter can be used as an analyser for measuring the degree of polarisation and phase of both diffuse and specular polarisation. The refractive index and the degree of polarisation can be physically determined by the zenith angle between the remitted light and the surface where the phase angle is determined by the azimuth angle of the remitted light to the surface. The surface orientation of a reflecting surface can be determined for a constant refractive index and vice versa by using the Fresnel theory of light, which is dictated by the polarisation nature of the incident light and the geometry of the scattering process. Polarisation information proves to be very useful for determining the surface quality by using refractive index estimation or surface shape for surfaces of constant refractive index.

The aim of this paper is mainly the computation of the refractive index of a material by using the Fresnel theory. Firstly, the method of moments is used which was proposed in [7] for moments estimates from multiple polarisation images. Secondly, photometric stereo is used for images taken with three different light source directions in order to determine the surface normals and consequently the angle of incidence for the incident light. Finally, the Fresnel theory for diffuse reflectance is used for estimating the refractive index. We use samples of fruits and vegetables at different stages of decay and surface texture to explore how effectively can the method be used for revealing local variations in refractive index.

2 Polarisation Image

For computing the components of the polarisation image, we follow the method that was proposed in [7] for diffuse reflectance using robust moment estimators, where light undergoes subsurface reflections before being re-emitted. The Fresnel theory gives the relationship between the degree of polarisation and the angle of reflection of the reflected light.

2.1 Data Collection

We collect a succession of images of the subject with different orientations of the analyser polaroid for measuring the polarisation state using the geodesic light dome[8]. The object is placed in the center of the geodesic light dome for image acquisition. We used a Nikon D200 digital SLR camera, with fixed exposure and aperture settings for obtaining the data set. An unpolarised light source has been used for the experiments where the images have been captured with the analyser angle being changed by increments of 10° to give 19 images per object.

Since the light source locations have been carefully calibrated, the use of the geodesic light dome gives accurate measures for the angle of incidence of the incident light source as shown in Figure (1) for a wrinkled apple, Figure (2) for an orange and Figure (3) for a tomato. The experiments are conducted in a dark room with matte-black walls hence, leading to minimal refelctions from the surroundings.

2.2 Robust Moments Estimators for Polarisation Image

The conventional way of estimating the components of the polarisation image, i.e. mean intensity, I_0, degree of polarisation, ρ, and phase, ϕ, has been to use the least-squares fitting of 3 images [9]. As has been mentioned earlier, we use the robust moments estimators for computing the components of the polarisation image from a larger set of data [7]. The method is explained as follows:

If the angle of the analyser is taken as β_i, where the index of the analyser angle is i. At the pixel indexed p with the analyser angle indexed i, the predicted brightness is

$$I_p^i = \hat{I}_p \Big\{ 1 + \rho_p \cos(2\beta_i - 2\phi_p) \Big\}. \tag{1}$$

where $\hat{I}_p$, ρ_p and ϕ_p are the mean intensity, polarisation and phase at the pixel indexed p.

We take N equally spaced polarisation images, where the polariser angle index is $i = 1, 2, ..., N$. To compute the polarisation parameters, we commence by normalising the pixel brightness values. Therefore,

$$x_p^i = (I_p^I - \hat{x}_p)/\hat{x}_p, \tag{2}$$

where

$$\hat{x}_p = 1/N \sum_{i=1}^{N} x_p^i. \tag{3}$$

At the pixel p the normalised brightness has variance: $\sigma_p^2 = 1/N \sum_{i=1}^{N} (x_p^i - \hat{x}_p)^2$. The moments estimators of the three components of the polarisation image are as follows:

$$\hat{I}_p = 1/N \sum_{i=1}^{N} I_p^I, \ \rho_p = \sqrt{2/\pi}\sigma_p \tag{4}$$

and

$$\phi_p = 1/2 \cos^{-1}(\langle \hat{x}_p \cos(2\beta_i) \rangle / \pi\rho_p). \tag{5}$$

3 Surface Normal Estimation

Photometric stereo has been used for estimating the angle of incidence for images acquired for three light source directions as has been proposed in [10] and further used in [11]. The mean-intensity component of the polarisation image has been used as input to the photometric stereo for computing the surface normals.

Let $S_m = (S_1|S_2|S_3)$ be the matrix with the three light source vectors as columns, N_p the surface normal at the pixel indexed p and $\hat{J}_p = (\hat{I}1_p, \hat{I}2_p, \hat{I}3_p)^T$ be the vector of the three mean brightness values recorded at the pixel indexed p with the three different light source directions. Under the assumption of Lambertian reflectance, at pixel p we have

$$\hat{J}_p = S_m N. \tag{6}$$

The surface normal can be calculated from the vector of brightness values J_p and the inverse of the source matrix S_m. The reflectance factor, R, is calculated by taking the magnitude of the right side of equation (7) because the surface normal, N, is assumed to have unit length

$$R_p = |[S_m]^{-1}\hat{J}_p|. \tag{7}$$

The unit normal vector is calculated as follows:

$$N = (1/R) * [S_m]^{-1}\hat{J}_p. \tag{8}$$

The images taken across the polarizer angles are reconstructed using the following equation:

$$J_p^i = S_m.N(1 + \rho_p cos(2\beta_i - 2\phi_p)). \tag{9}$$

The surface normal information is used to compute the angle of incidence of the incident light, which is given by the dot product of the source vector and the surface normal.

4 Refractive Index Estimation

Fresnel theory of light predicts that light incident on a surface is partially polarised and refracted while penetrating the surface. Scattering due to the structure of the reflecting surface depolarises the incident light. The remitted light is refracted into the air and hence is refracted and partially polarised in the process. From the Fresnel theory of light, the relationship between the degree of diffuse polarisation, the angle between the surface normal and the remitted light θ and the refractive index n is given as follows:

$$\rho = \frac{(n-\frac{1}{n})^2 \sin^2\theta}{2+2n^2-(n+\frac{1}{n})^2\sin^2\theta+4\cos\theta\sqrt{n^2-\sin^2\theta}}. \tag{10}$$

If ρ and θ are known then the above equation can be solved for the refractive index n. The refractive index is given by the roots of quartic equation:

$$A^2n^4 + (2AC-1)n^3 + (2AB + C^2 + \sin^2\theta)n^2 + 2BCn + B^2 = 0. \tag{11}$$

where $A = ((1+\rho)\sin^2\theta - \frac{2\rho}{4\rho\cos\theta})$, $B = (\frac{(1+\rho)\sin^2\theta+\rho}{4\rho\cos\theta})$ and $C = -\frac{2((1-\rho)\sin^2\theta+\rho)}{4\rho\cos\theta}$. In practice, we find that only one root falls within the physical range of refractive index

encountered for biological tissue, i.e. $1 < n < 2.5$. For specular polarisation, there is a similar equation but its solution requires only the solution of a cubic equation in refractive index [12]. We have used the Newton-Raphson method to compute the roots of the equation (11), 10 iterations have been used to get the final value for the refractive index.

There are other methods that have been proposed for estimating the refractive index, which are as follows: multi-spectral polarisation imagery from a single viewpoint [13], the spectral dependence of the refractive index has been studied in [14], [15], [16]. Our method differs from these as we have used the Fresnel theory in conjunction with photometric stereo and estimates of the polarisation image from the robust moments estimator for estimating the refractive indices.

5 Experiments

As has been already mentioned the images were acquired in a dark room. The objects and the camera are positioned on the same axis while the LED (light sources) are positioned at different angles in the geodesic light dome designed by Cooper et al. for controlling the light sources while the camera operation is manual [8]. A linear polarising filter is placed in front of the camera lens where the orientation is changed manually. The experiments were carried out on a wrinkled apple, orange and tomato. The orange

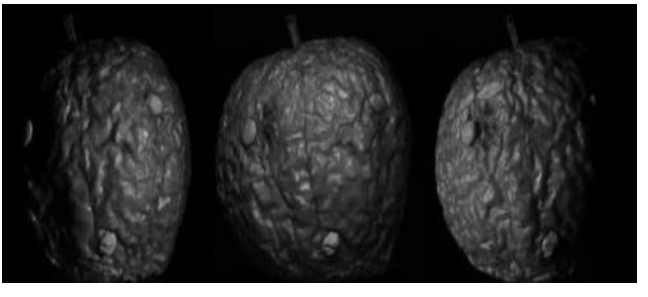

Fig. 1. The scene for a wrinkled apple using three different light source directions

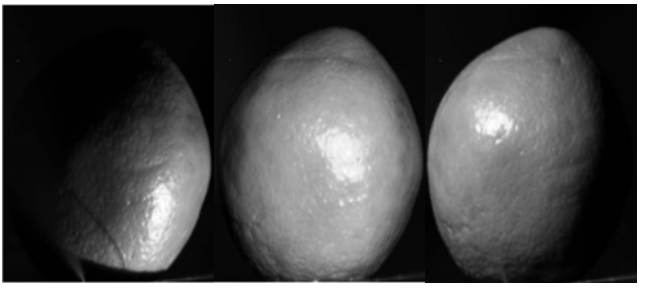

Fig. 2. The scene for an orange using three different light source directions

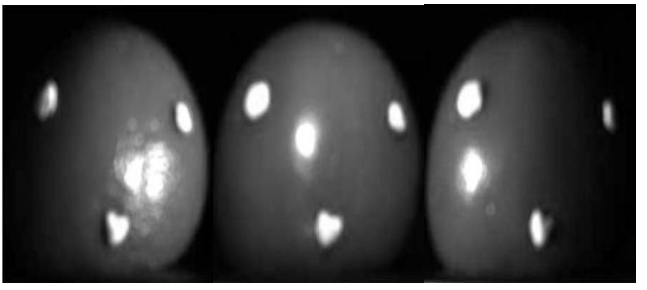

Fig. 3. The scene for a tomato using three different light source directions

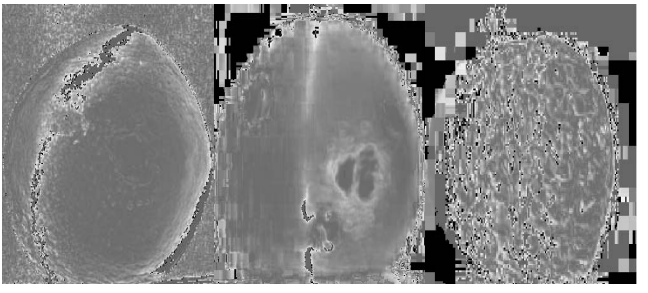

Fig. 4. The refractive index images for an orange, tomato and apple, respectively

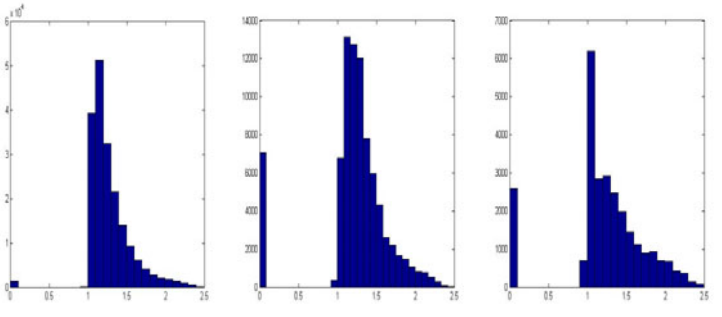

Fig. 5. The histograms for an orange, tomato and apple, respectively

has been chosen in order to test the method due to presence of natural indentations in the surface. We have placed lumps of blu-tac on the surface of the apple. The aim here is to detect whether the method can deal with local variations of shape and refractive index. For the three objects the values for the refractive indices fall in the range $1 < n < 2.5$. There are some outliers which have been filtered. These mainly correspond to non-physical values of the refractive index, which are less than unity. The refractive index images for the different objects are shown in Figure (4). From the images it is clear that

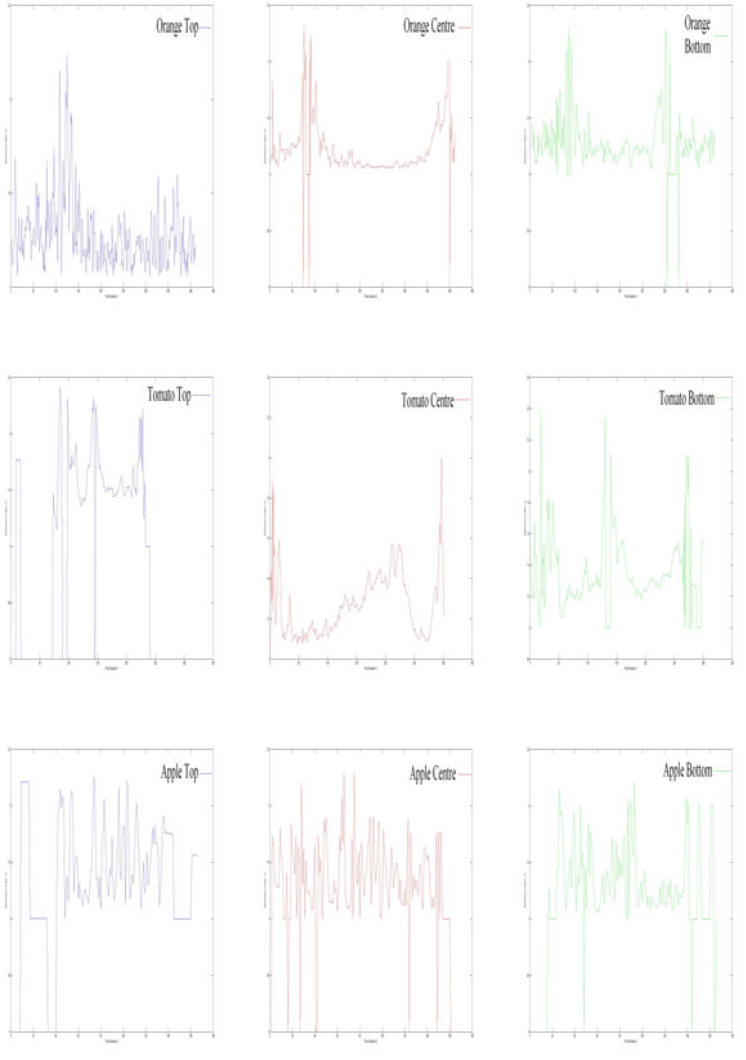

Fig. 6. [Top to Bottom]The top, centre and bottom profiles of an orange, tomato and apple, respectively

the blu-tac on the apple can be detected as both changes in shape and refractive index. Also, regions of specularity have refractive index $'0'$ since, we use the Fresnel equation for the diffuse reflectance. Figure (5) shows histograms of the refractive indices for the apple, tomato and an orange. The modal values are consistent with tabulated values for the refractive index, and the non physical outliers are well separated from the main distribution. Figure. (6) shows refractive index profiles across the physical top, centre

and bottom for each object. For the apple and tomato, the profiles are flat, showing that there is no residual shape-bias in the estimation of refractive index. However, the profiles for the orange shows significant variation near the object boundary, and this may be attributable to its indented surface and the boundary effects of roughness. However, the profiles are quite stable in the centre of the object. Infact the profiles of all of the object, show more variation near the boundaries and also where there is a change of material (e.g. the blu-tac lumps). In the case of the apple where the surface is wrinkled due to loss of water content and rotting, there is variation in refractive index.

It is worth mentioning that there are potential sources of error in the computation of the refractive indices because the surface for the apple is wrinkled. This has resulted in inter-reflections and these in turn lead to unrealistic values. On the other hand, the tomato is smooth apart from where there is a change of material where the blue-tac lumps have been added. This change of composition is enhanced in the refractive index image. For the orange the dents in the skin appear as refractive index variations, probably due to inter-reflections and sub-surface reflections. There is also the possibility of error due to noise and camera jitter. Also, the degree of polarisation computations might not be accurate due to misalignment of the polariser angles.

6 Conclusions

In this paper we have exploited the information that is acquired from the Fresnel theory and polarisation information for refractive index estimation. Our approach has been to use information from the polarisation image computed using robust moments estimation and surface normal estimation using photometric stereo. These results are used as inputs to the Fresnel equation for diffuse reflectance, in order to compute the refractive index of the material. The computation is considered to be effective since the refractive indices vary with the change in material and do not exhibit significant shape bias.

References

1. Dunn, A., Richards-Kortum, R.: Three-Dimensional Computation of Light Scattering From Cells. IEEE Journal of Selected topics in Quantum Electronics 2(4) (1996)
2. Saidi, I., Jacques, S., Kittel, F.: Mie and Rayleigh modeling of visible-light scattering in neonatal skin. Applied Optics 34, 7410–7418 (1995)
3. Yee, K.: Numerical Solutions of initial boundary value problems involving Maxwell's equations in instotropic media. IEEE Transactions on Antennas Propagation AP-14, 302–307 (1966)
4. Hecht, E.: Optics, 4th edn. Addison-Wesley, Reading (2002)
5. Wolff, L.B., Boult, T.E.: Constraining Object Features using a Polarisation Reflectance Model. IEEE Transactions on Pattern Analysis and Machine Intelligence 13, 635–657 (1991)
6. Born, M., Wolf, E.: Principles of Optics, 7th edn. Cambridge University Press, Cambridge (1999)
7. Saman, G., Hancock, E.R.: Robust Computation of the Polarisation Image. In: International Conference on Pattern Recognition (2010)

8. Cooper, P., Thomas, M.: Geodesic Light Dome. Department of Computer Science, University of York, UK (March 2010), http://www-users.cs.york.ac.uk/-pcc/Circuits/dome (accessed on: September 10, 2010)
9. Atkinson, G., Hancock, E.R.: Robust estimation of reflectance functions from polarization. Springer, Heidelberg (2007)
10. Woodham, R.J.: Photometric method for determining surface orientation from multiple images. Optical Engineering 19(1) (1980)
11. Coleman, E.N., Jain, R.: Obtaining 3-Dimensional Shape of textured and Specular surfaces using four-source photometry. Computer Graphics and Image Processing 18(4), 309–328 (1982)
12. Atkinson, G., Hancock, E.R.: Recovery of Surface Orientation from Diffuse Polarization. IEEE Transactions on Image Processing 15(6) (2006)
13. Huynh, C.P., Robles-Kelly, A., Hancock, E.R.: Shape and Refractive Index Recovery from single-view polarisation images. In: IEEE Conference on Computer Vision and Pattern Recognition (2010)
14. Chang, H., Charalampopoulos, T.T.: Determination of the wavelength dependence of refractive indices of flame soot. Royal Society (1990)
15. Bashkatov, A.N., Genina, E.A., Kochubey, V.I., Tuchin, V.V.: Estimation of wavelength dependence of refractive index of collagen fibers of scleral tissue. In: Proceedings of SPIE, vol. 4162, p. 265 (2000)
16. Ding, H., Lu, J.Q., Wooden, W.A., Kragel, P.J., Hu, X.: Refractive indices of human skin tissues at eight wavelengths and estimated dispersion relations between 300 and 1600nm. Journal Physics in Medicine and Biology 51(6) (2006)